

SIMULTANEOUS OBSERVATIONS OF *COMPTON GAMMA RAY OBSERVATORY*–*BATSE* GAMMA-RAY BURSTS WITH THE *COBE* DMR

PETER D. JACKSON

Raytheon STX Corporation, NASA Goddard Space Flight Center, Greenbelt, MD 20771; pjackson@picasso.gsfc.nasa.gov

CHRISTOPH WINKLER

ESA/ESTEC Astrophysics Division, P.O. Box 299, NL-2200 AG Noordwijk, The Netherlands; cwinkler@ests2.estec.esa.nl

J. GREGORY STACY¹

Department of Physics and Astronomy, Louisiana State University, Baton Rouge, LA 70803; gstacy@rouge.phys.lsu.edu

AND

TJ. ROMKE BONTEKOE²

Bontekoe Data Consultancy, Herengracht 47, NL-2312 LC Leiden, The Netherlands; romke@astro.uva.nl

Received 1997 March 27; accepted 1998 April 24

ABSTRACT

Data acquired with the *COBE* Differential Microwave Radiometer (DMR) provide a unique opportunity to observe simultaneous emission from cosmic gamma-ray bursts in the previously unexplored microwave region of the spectrum. We have searched the *COBE* DMR time-ordered data sets for instances when one of the DMR horns (FWHM $\sim 7^\circ$) was pointing in the direction of a gamma-ray burst at the time of burst occurrence. During the overlap period 1991 April–December corresponding to the first public release of *COBE* data, 210 *Compton Gamma Ray Observatory* (CGRO)/*BATSE* gamma-ray bursts listed in the Third *BATSE* (3B) Catalog were viewable by the *COBE* DMR. For five of these events the DMR was pointing within 7° of the burst positions at the exact moment of burst occurrence. For another four events the DMR was pointed within 2° of the *BATSE* positions within 10 s of the burst trigger time. No obvious microwave emission (at 31.5, 53, or 90 GHz), with upper limits in the 10–100 kJy range, can be associated with any of these events. The *COBE* DMR has a relatively low sensitivity for the detection of point sources within its field of view. A positive detection of a gamma-ray burst by the *COBE* DMR would imply that the integrated microwave flux must be of the same order as the energy observed in gamma rays. By extending an acceptance window in time of up to 20 minutes before and after a gamma-ray burst another 60 bursts are sampled by the DMR, whose signals are analyzed statistically. We conclude that the “average” gamma-ray burst produces less than about 7–42 kJy in simultaneous microwave radiation.

Subject headings: cosmic microwave background — gamma rays: bursts —
radiation mechanisms: nonthermal — radio continuum: general

1. INTRODUCTION

Ever since gamma-ray detectors have been in space, occasional, intense transient events of gamma-ray emission, termed gamma-ray bursts (GRBs), have been detected, lasting from milliseconds to minutes (Klebesadel, Strong, & Olsen 1973). Since the launch of the *Compton Gamma Ray Observatory* (CGRO) in 1991, the Burst and Transient Source Experiment (*BATSE*), the first large-scale gamma-ray instrument designed expressly to study such phenomena, has been observing numerous GRBs, over 2000 to date, with accurate timing and a positional accuracy of 1 to several degrees (Fishman et al. 1994; Meegan et al. 1996). Despite this formidable collection of information on bursts and their properties, no correlation of GRB positions with any class of objects, within or outside the Galaxy, has been substantiated. And, until very recently, no counterpart emission at other wavelengths (radio through X-rays), simultaneous or quiescent, has been observed for any GRB (e.g., Fishman 1995; Greiner 1995; Vrba 1996), leading to

considerable debate on the distance scale to the sources of GRBs (see Paczyński 1995; Lamb 1995). Recently, however, major progress in understanding the GRB phenomenon has been made through the identification of counterparts at X-ray, optical, and radio wavelengths, following the precise location of a small number of GRBs by the Italian-Dutch *Beppo-SAX* X-ray satellite (e.g., Costa et al. 1997). These latest results offer the most compelling evidence to date that the sources of GRBs lie at cosmological distances and that the observations can be readily explained in terms of simple relativistic fireball models (Metzger et al. 1997; Wijers, Rees, & Mészáros 1997). Here we describe a separate, independent effort to search for counterparts to GRBs at microwave energies, based on a number of serendipitous, simultaneous observations of GRBs with the Differential Microwave Radiometer (DMR) instrument aboard the *Cosmic Background Explorer* (*COBE*) satellite.

The primary goal of the DMR instrument was to map the cosmic background radiation over the entire sky. All-sky maps of the microwave background radiation were produced by fitting the recorded differential radiometer data to a pixelated representation of the sky (see Jackson et al. 1992; Keegstra et al. 1992; Bennett et al. 1994, 1996). However, for the present application we do not make use of these skymaps. Rather, we attempt to detect the microwave flux

¹ Also, Department of Physics, Southern University, Baton Rouge, LA 70813.

² Also, Astronomical Institute “Anton Pannekoek,” University of Amsterdam, The Netherlands.

from a point source at a known position at a given instant. Our analysis makes use of the calibrated DMR time-ordered data (TOD) around the times of BATSE burst triggers. At these times the DMR radiometer pointings on the sky are compared with known burst positions as listed in the Third BATSE (3B) Catalog of Meegan et al. (1996). When coincident, the recorded DMR flux density is assigned to the GRB under the assumption that the second horn of the radiometer, which is pointing in another direction, receives no signal. A search is then carried out for significant transient microwave emission above the rms noise level of the DMR that might be ascribed to the GRB.

At any given instant, the DMR observes almost 300 deg^2 of the sky, so there is a $\sim 0.7\%$ chance that a particular GRB will be observed by the DMR at the time of burst occurrence. With a burst rate of about one per day, one expects a few GRBs per year to occur within the field of view of the DMR at one of its three frequencies. This number increases if one allows an acceptance window around the times of bursts (to search for “precursor” or “afterglow” microwave emission, for example). In this investigation, we have analyzed the DMR data over a time period of 40 minutes centered on the burst trigger times. We did not analyze the DMR data beyond 20 minutes before or after burst occurrence, since the results of such analyses have been presented elsewhere (Ali et al. 1997; Schaefer et al. 1995) and ground-based observing programs have made searches at the larger time differences to much lower flux limits than we can achieve with the DMR data (e.g., Frail et al. 1997).

Here we present the results of our analysis for the first overlap period in publicly released data sets for the *COBE* and *CGRO* missions, 1991 April–December. A second public release of DMR data has recently occurred, covering the period up to 1993 December. Our analysis of these later data sets will be the subject of a follow-up report.

2. DMR OBSERVATIONS AND ANALYSIS

The DMR instrument has been described elsewhere (e.g., Smoot et al. 1990; Bennett et al. 1992, 1994, 1996). Here we concentrate on features that are relevant to the detection of discrete sources at known positions.

The DMR operates at three frequencies: 31.5, 53, and 90 GHz. For each frequency there are two independent radiometers, or channels. Each channel receives the signals from two horns, with their pointing directions separated by 60° . The beamwidths of the horns are about 7° between half-power points. With a spacecraft spin period of 75 s, the radiometers move across the sky at a rate of about 2.5 s^{-1} . Thus, in one complete revolution a given point on the sky will be viewed, at 12.5 s intervals, in succession by the first horn of the 31.5, 90, and 53 GHz radiometers and then by the second horn of the same 31.5, 90, and 53 radiometers. In 12.5 s the DMR horns have covered, without overlap, 1260 deg^2 of sky, giving a 3% chance that a GRB would be observed during that period, if one occurred. Because of the orbital motion of the *COBE* spacecraft, a point on the sky remains visible to the DMR for about two complete spin revolutions. The *COBE* spacecraft orbits with a period of 102 minutes. The sky coverage of the combined orbital and spin motion is a 67° wide annulus on the sky.

A consequence of the large sky coverage of the DMR is a relatively low sensitivity to point sources. Furthermore, since the instrument was only passively cooled to about

140 K, the radiometer noise temperatures are comparatively high. The differential signal, or more precisely the differential antenna temperature, is obtained by switching at a rate of 100 Hz between the two horns of each channel. The telemetry data consist of integrated differential antenna temperatures, taken with an integration time of 0.5 s (a minor frame of telemetry). Table 1 gives the rms noise levels of the DMR radiometers, expressed in millikelvins of antenna temperature and in Janskys of flux (S), at each frequency for both a 0.5 and 1.5 s integration interval (the latter figure refers to the time it takes a point source to pass through half of the DMR beam). The antenna temperature noise levels were taken from Bennett et al. (1992) and were decreased by 3.2% since we are not applying a correlation memory correction that was applied in the standard data processing for the *COBE* mission. The corresponding noise levels in Janskys are based on beam solid angles of about 70 deg^2 for each horn. Even with these relatively high rms noise levels, the flux limits derived from DMR observations of GRBs are still of astrophysical interest for two reasons. First, they represent the first truly simultaneous observations of GRBs at microwave frequencies. And second, the all-sky coverage achieved by the DMR over the course of the *COBE* mission is not yet feasible with ground-based telescopes.

The DMR TOD contain baseline and gain corrections for converting the digitized intensity counts into millikelvin antenna temperature. We follow the same baseline correction procedure employed in the standard DMR mission processing (Bennett et al. 1994). To ensure that there is no net sky emission in the TOD, we subtracted both the 3 mK cosmic background dipole radiation, as well as the 2 yr *COBE* DMR mission skymaps, from the data. By subtracting the skymaps, we eliminate any effects of diffuse emission from the Galaxy. The total of these corrections is typically $\sim 3 \text{ mK}$, with a maximum of $\sim 9 \text{ mK}$ toward the Galactic center at 31 GHz. We make no corrections for magnetic susceptibility, instrument memory, Earth velocity, satellite velocity, or off-axis lunar emission since these effects are not important for the relatively short integration times considered for this paper. We also rejected any TOD flagged for bad attitude solutions or bad telemetry. However, we accepted data flagged as “Earth close” and “Moon close” (except when the Moon was obviously affecting the data). We inspected data flagged as “spike” (being more than 5 standard deviations from the mean) to be sure that it might not be a real burst of emission from the

TABLE 1
RMS UNCERTAINTY IN THE MEASUREMENT OF MICROWAVE EMISSION
FROM A POINT SOURCE WITH THE *COBE* DMR

DMR Channel	T_a (mK)	S (kJy) (0.5 s Integration)	S (kJy) ^a (1.5 s Integration)
31A	56.8	36.4	15.1 (21.0) ^b
31B	58.5	37.5	...
53A	22.5	40.8	17.9
53B	26.3	47.7	...
90A	38.5	213	71.8
90B	29.3	153	...

^a Averaged over both frequency channels.

^b After 1991 October 4, the 31B radiometer became very noisy for almost a year, so only channel 31A could be used with an rms uncertainty of 21.0 kJy.

sky. However, no such spikes occurred simultaneously in both frequency channels as would be the case for a real burst. Finally, since the DMR beam takes approximately 1.5 s to cross a point in the sky, we averaged the data into 1.5 s bins and also averaged over both channels for each frequency. Included in Table 1 is the rms uncertainty of the flux from a point source after this averaging of the data.

Since the Moon is the only source that can be directly seen in the DMR TOD in a single pass of the DMR, we tested our analysis software by adding the Moon to our input list of candidate BATSE bursts, at a position and time when it was known to be viewable by the DMR. Our searching algorithm properly identified the Moon as a burstlike “simultaneous event” in the TOD at the correct position and time.

3. RESULTS

3.1. Simultaneous Events

Two preliminary reports of this work (Bontekoe et al. 1995; Stacy et al. 1996) were based on GRB positions taken from the First BATSE (1B) Catalog of Fishman et al. (1994) and cited the simultaneous observation of GRB 911226 by the *COBE* DMR and a search over a BATSE-DMR time difference window of 40 minutes. Late in 1995, the 3B Catalog was released (Meegan et al. 1996), and, while positions for strong GRBs changed very little, the positions of a number of weaker GRBs changed considerably. In particular, the position of GRB 911226 was revised by about 9°, effectively moving it out of the DMR beam. The results reported here are all based on the latest positions of the 3B Catalog.

Of the 210 BATSE events during the overlap period from 1991 April to December, the DMR was pointing within 7° (i.e., within the half-power beamwidth of the DMR beam) of the positions of five GRBs at the BATSE trigger time. Furthermore, the DMR was pointing within 2° of the BATSE positions of an additional four events within 10 s of the BATSE burst trigger. The most interesting of the DMR-BATSE coincident observations are for those GRBs with (1) a high gamma-ray fluence and hence a small error in the 3B position and (2) a BATSE position close to the center of the DMR beam at the moment of burst occurrence. Our best candidates for detailed study are the GRBs 910709 (BATSE trigger number 503), 911111B (number 1046), and 911224B (number 1212). A summary of the DMR observations of these and other GRBs in our sample that fall within the beam of one of the DMR horns within 30 s of the BATSE trigger time is given in Table 2. The observed DMR flux is listed, by frequency, in terms of time and position difference. No significant microwave emission, with upper limits in the 10–100 kJy range, can be associated with any of these simultaneous and near-simultaneous events. A summary of the gamma-ray properties of these BATSE bursts, as extracted from the 3B Catalog, is given in Table 3. We have used the burst location error models adopted by the BATSE team (Briggs et al. 1998) to calculate the 99% confidence error radii listed in Table 3.

The general spectral and temporal characteristics of these bursts, as derived from observations with the BATSE and COMPTEL instruments aboard the *CGRO*, do not show any extraordinary properties in the hard X-ray through medium gamma-ray range. For our three primary candidate events they can be briefly summarized as follows.

TABLE 2
DMR OBSERVATIONS OF BATSE BURSTS WITHIN 30 s
OF BURST TRIGGER

Burst Name	Δt^a (s)	Δr^b (deg)	DMR Flux ^c (rms)	Frequency (GHz)
3B 910518	22.5	6.9	0.35	31
3B 910701	7.5	6.5	-0.06	31
	19.5	6.0	-0.29	90
	21.0	6.9	1.06	90
3B 910705	28.5	6.7	-1.49	31
3B 910709	-28.5	6.5	0.75	53
	-27.0	3.3	0.33	53
	-25.5	1.8	0.26	53
	-24.0	4.5	0.92	53
	-16.5	6.5	-0.36	31
	-15.0	3.4	-0.34	31
	-13.5	2.0	0.08	31
	-12.0	4.6	-0.48	31
	-3.0	4.9	1.05	90
	-1.5	2.2	1.42	90
	0.0	3.1	1.75	90
	1.5	6.2	0.12	90
	10.5	3.9	0.57	53
	12.0	1.8	0.56	53
	13.5	3.9	-1.43	53
	22.5	5.4	-0.98	31
	24.0	2.6	-0.70	31
	25.5	2.9	0.37	31
	27.0	5.9	1.07	31
3B 910826	-15.0	6.7	0.20	53
	-27.0	5.5	-0.16	90
	-25.5	6.2	0.40	90
	-13.5	6.2	0.89	53
	-1.5	6.4	0.56	31
3B 910828	12.0	6.7	2.29	31
	24.0	6.2	-0.95	90
	25.5	6.7	0.84	90
3B 910912	-25.5	6.9	0.95	31
	-24.0	3.3	-0.04	31
	-22.5	0.5	0.70	31
	-21.0	4.2	-0.10	31
	-13.5	6.9	0.17	90
	-12.0	3.2	0.90	90
	-10.5	0.7	-0.12	90
	-9.0	4.4	1.26	90
	0.0	4.0	1.17	53
	1.5	1.7	-0.19	53
	3.0	4.3	0.53	53
	12.0	3.7	0.60	31
	13.5	2.5	0.36	31
	15.0	5.3	-1.32	31
	24.0	4.9	2.16	90
	25.5	3.0	-0.04	90
	27.0	4.9	-1.80	90
3B 911111B.....	-28.5	6.6	-0.97	53
	-27.0	3.2	-0.03	53
	-25.5	2.5	-0.34	53
	-24.0	5.5	0.77	53
	-16.5	5.6	-1.02	31
	-15.0	2.2	-1.05	31
	-13.5	2.5	-0.02	31
	-12.0	6.0	0.31	31
	-4.5	6.4	0.12	90
	-3.0	2.7	1.04	90
	-1.5	1.2	-0.92	90
	0.0	4.8	0.04	90
	9.0	4.1	0.32	53
	10.5	0.5	-0.36	53
	12.0	3.2	-0.46	53
	13.5	6.9	0.42	53
	21.0	4.7	1.23	31
	22.5	1.5	1.29	31
	24.0	3.0	-0.04	31
	25.5	6.5	0.30	31

TABLE 2—Continued

Burst Name	Δt^a (s)	Δr^b (deg)	DMR Flux ^c (rms)	Frequency (GHz)
3B 911123B.....	-22.5	6.4	-0.13	31
	-21.0	6.9	0.86	31
	-10.5	6.6	0.06	90
3B 911124	15.0	6.9	-0.68	31
	27.0	6.1	0.68	90
3B 911224B.....	-27.0	6.6	-1.34	90
	-25.5	2.9	2.41	90
	-24.0	1.0	-0.02	90
	-22.5	4.7	2.10	90
	-15.0	6.7	-0.17	53
	-13.5	3.0	1.79	53
	-12.0	0.8	0.44	53
	-10.5	4.5	0.77	53
	-3.0	5.6	0.22	31
	-1.5	1.9	0.87	31
	0.0	2.0	0.68	31
	1.5	5.7	-0.56	31
	9.0	6.3	-1.02	90
	10.5	2.6	1.27	90
	12.0	1.4	0.39	90
	13.5	5.0	1.22	90
	22.5	3.9	1.08	53
	24.0	1.0	0.43	53
	25.5	3.9	0.24	53
3B 911226	-21.0	5.7	0.37	31
	-19.5	5.9	1.61	31
	-9.0	5.6	0.63	90
	-7.5	5.3	0.79	90
	3.0	6.1	-2.12	53
	4.5	4.7	0.50	53
	6.0	6.2	-0.75	53
	15.0	5.6	-0.51	31
	16.5	4.0	-1.57	31
	18.0	5.6	0.15	31
	27.0	5.0	-0.59	90
	28.5	3.7	1.24	90

^a The difference in time between the BATSE trigger time and the DMR (negative values indicate DMR flux readings prior to burst occurrence).

^b The angular distance between the BATSE 3B position for the burst and the current pointing direction of the closest DMR horn of the given frequency.

^c DMR Channels A and B have been combined; the flux values are in units of rms uncertainty (see Table 1) for an integration time of 1.5 s (the time required for a source to pass through half of the DMR beam).

The BATSE burst GRB 910709 lasted for 1 s and was also detected by the medium-energy (0.8–30 MeV) COMPTEL instrument aboard the *CGRO*. The gamma-ray

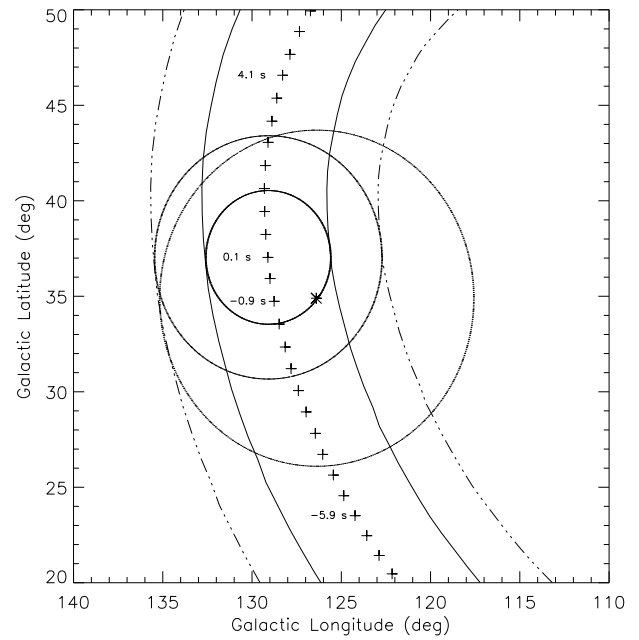


FIG. 1.—A sky map showing the field containing the 3B burst GRB 910709. Also shown are the successive positions of the beam of one of the 90 GHz horns of the DMR, illustrating that this GRB was within the DMR beam at the moment of burst occurrence. The asterisk marks the position of 3B GRB 910709, centered within the BATSE 99% confidence error circle. Plus symbols (+) mark the positions of the DMR horn at the midpoint of each 0.5 s integration period. Some of the plus symbols are labeled with the difference (in s) between the DMR sampling times and the BATSE trigger time. The concentric circles centered on the DMR position closest in time to the burst trigger time (at +0.1 s) show the FWHM and “10% sensitivity” levels of the circular Gaussian DMR beam (cf. Fig. 6 of Bennett et al. 1992). The solid and dash-dotted lines indicate the boundaries of the DMR beam as it sweeps across the field. The moment of “closest approach” by this DMR horn to the burst position occurred at -0.9 s, just before burst occurrence.

spectral shape for this event is characterized by a power law of index -2.9 over a range from 1 to 10 MeV (Kippen 1995; Hanlon et al. 1994). Figure 1 shows a sky map of the field containing GRB 910709, with the path of the DMR beam superposed. Several of the DMR pointing directions are labeled with the time difference with respect to the burst trigger time, demonstrating that GRB 910709 was within the 90 GHz beam of the DMR at the moment of burst occurrence.

GRB 911111B has a well-defined gamma-ray light curve

TABLE 3

SELECTED GAMMA-RAY PROPERTIES OF GRBS OBSERVED WITH THE *COBE* DMR WITHIN 30 s OF BURST TRIGGER

GRB Name (3B)	BATSE Trigger Number	Position Error (99%) ^a (deg)	Duration 5%–95% (s)	Fluence > 20 keV ($\times 10^{-7}$ ergs cm^{-2})
910518	207	9.6	0.08	4.0 ± 1.2
910701	472	23.1	82.	$40.0 \pm 19.$
910705	491	18.3	0.1	12.0 ± 1.7
910709	503	8.8	46.	57.7 ± 2.4
910826	727	10.8	...	13.9 ± 2.8
910828	734	12.9	1.8	8.8 ± 3.8
910912	788	15.7	0.3	1.43 ± 0.5
911111B	1046	9.3	114	74.1 ± 8.8
911123B	1112	9.6	0.44	15.3 ± 1.0
911124	1118	10.4	...	38.2 ± 4.4
911224B	1212	12.1	...	$83.8 \pm 17.$
911226	1223	16.3	1.	< 3.6

^a The burst location error models adopted by the BATSE team (Briggs et al. 1998) were used to compute the 99% confidence error radii listed.

of medium strength and exhibits gamma emission up to about 60 s after onset. GRB 911224B also has a well-defined light curve, with three subpulses and about 50 s of total emission. Interestingly, this GRB also shows precursor gamma-ray emission of approximately 10 s duration starting at about 75 s before the main BATSE trigger. Analysis of the DMR data for all three of these bursts was extended to 300 s before and after the BATSE trigger times, but no significant microwave emission was detected that could be attributed to the bursts.

In summary, we show in Figure 2 the microwave flux recorded by the DMR as a function of DMR-BATSE time for all 12 GRBs (see Table 3) that fall within the beam of one of the DMR horns within 30 s of the burst trigger time. Flux is given in units of rms uncertainty so that all three DMR frequencies can be represented on the same plot. For these individual GRBs, no significant microwave emission is detected by the *COBE* DMR around the time of the burst.

3.2. Cumulative Results

To search for possible weak quiescent, precursor or afterglow microwave emission from GRBs as a class, we extended our analysis by expanding the acceptance time window for BATSE-DMR coincidences to 40 minutes around the time of a BATSE burst. A total of 60 GRBs from our sample fall within the 7° wide beam of one of the DMR horns within 20 minutes before or after the BATSE trigger time. Examination of the “phase space” plot of the observed DMR flux density versus BATSE-DMR time difference for all 60 GRBs shows that it is nearly uniformly filled, implying that there are no obvious gaps in the DMR sampling of burst time histories. Nor are there any evident regions of oversampling, implying that statistical averaging techniques can be applied to the collective data to derive the microwave properties of an “average” burst.

By combining the flux-versus-time profiles for all 60 GRBs and averaging over relatively large time bins, one artificially obtains a higher sensitivity to small but systematic signatures in the microwave emission from GRBs on timescales comparable to the bin size. However, we find no

collective microwave signature in our sample of 60 GRBs. Plots and histograms for the case of DMR flux averaged into 100 s time bins can be found in Stacy et al. (1996). We conclude from this procedure that the “average” GRB emits less than about 7 kJy (31.5 GHz), 9 kJy (53 GHz), and 42 kJy (90 GHz) of microwave emission.

The limits cited above are corrected for the fact that most GRBs are observed by the DMR at an off-axis angle. In the earlier reports of Bontekoe et al. (1995) and Stacy et al. (1996), all flux densities and limits were given as if the sources were observed on the axes of the DMR horns, the direction of highest sensitivity. For off-axis positions a correction should be made for the approximately Gaussian sensitivity profiles of the DMR. For example, if a GRB passed 3.5° away from the axis, the DMR sensitivity decreases by a factor 2.

Applying the burst location error models adopted by the BATSE team (Briggs et al. 1998) to a representative sample of bursts, we have calculated a mean uncertainty in the 3B burst positions of 7.1° . We estimate that the combined effect (of the off-axis DMR response and the burst location uncertainty) corresponds to a mean DMR-GRB separation of approximately 8.2° . The statistical correction for the flux densities observed off of the main axis of the DMR beam is then a factor of 14. We have applied this correction to the flux-density scales to obtain the limits cited above.

4. DISCUSSION

It has long been recognized that the key to unraveling the GRB mystery is the identification of a burst counterpart at another wavelength. The short duration of gamma-ray bursts, however, combined with the unpredictability of their occurrence anywhere in the sky and the relatively poor location determination capabilities of the gamma-ray instruments originally designed to detect them, has historically severely limited the effectiveness of coordinated follow-up searches for GRB counterparts. An observational breakthrough was achieved in early 1997 after the launch of the Italian-Dutch *Beppo-SAX* X-ray satellite (Piro, Scarsi, & Butler 1995). With its wide-field X-ray cameras the *Beppo-SAX* satellite has serendipitously observed the X-ray afterglow from a small number of gamma-ray bursts (e.g., Costa et al. 1997), which has resulted in the first detections of gamma-ray burst counterparts at optical and radio wavelengths (van Paradijs et al. 1997; Frail et al. 1997). We summarize briefly below the results associated with the *Beppo-SAX* satellite.

The first detection of transient X-ray and optical emission from a GRB was reported for the event of 1997 February 28 (Costa et al. 1997; van Paradijs et al. 1997). Follow-up observations of the fading optical counterpart to GRB 970228 with the *Hubble Space Telescope* (Sahu et al. 1997) indicated that the optical transient was associated with a faint extended source, suggestive of a very distant host galaxy. Further evidence for a likely cosmological origin for GRBs was obtained with the detection of both optical and radio counterparts to the gamma-ray burst of 1997 May 8 (Djorgovski et al. 1997; Frail et al. 1997). In this instance, absorption features measured in the spectrum of the fading optical emission associated with GRB 970508 indicated a redshift of approximately 0.8 to the absorbing material (Metzger et al. 1997). Interferometric radio observations at 1.43, 4.86, and 8.46 GHz with the VLA by Frail et al. (1997) showed a fluctuating radio source at the same position. At

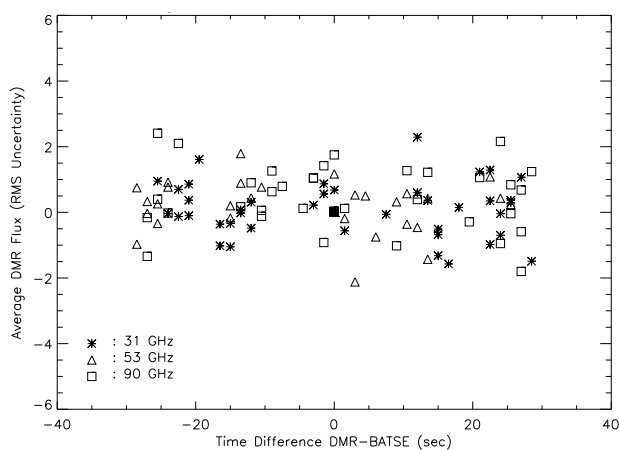


FIG. 2.—A plot of the average DMR flux as a function of time for the 12 BATSE gamma-ray bursts listed in Table 3 for which one of the DMR horns was pointed within 7° of the BATSE 3B position within 30 s of the burst trigger time. Each frequency is represented by a different symbol. The data have been averaged over 1.5 s, the time required for a source to pass through half of the DMR beam. The flux values are expressed in units of rms uncertainty averaged over a 1.5 s integration time and over both frequency channels (see Table 1).

4.86 and 8.46 GHz the source was detected when first observed (5–6 days after burst occurrence), with peak intensities of ~ 1.2 – 1.4 mJy at these frequencies noted about 20 days after burst occurrence and with average flux values in the range 0.5–0.7 mJy. The apparent damping of flux variations with time is consistent with diminished interstellar scattering of the radio emission from an expanding source. Additional VLBA observations of the radio counterpart of GRB 970508 allowed precise limits to be placed on the proper motion of the radio source, ruling out a very local origin for the radio emission (> 1 kpc; Taylor et al. 1997).

The dramatic results associated with *Beppo-SAX* offer the most compelling evidence to date that GRBs originate at cosmological distances (with characteristic redshifts of $z \sim 1$). This conclusion is further strengthened by earlier measurements suggesting that fainter bursts tend to evolve more slowly (because of time dilation effects stemming from the relativistic recession velocity), implying that the sources of GRBs must be cosmologically distant (Norris et al. 1995). This likely determination of the GRB distance scale has permitted a serious reevaluation of the many theories put forward to explain the origin of GRBs. The class of model generally favored at present is that of the “relativistic fireball,” which posits an enormous, instantaneous energy release within a small volume (see, for example, Wijers et al. 1997). In such a scenario, the delayed onset and characteristic decay observed for the counterpart emission at X-ray, optical, and radio wavelengths can be naturally explained as arising from shocks associated with a relativistically expanding pair plasma that becomes progressively more optically thin to lower frequency radiation during the later stages of the development of the cooling fireball. The exact details, however, of the broadband emission properties depend critically on the interstellar or intergalactic environment within which the explosive event occurs (see, for example, Waxman 1997). A related question is the nature of the “trigger” that sparks the detonation of the fireball itself. The enormous energies ($\geq 10^{51}$ ergs) implied by the cosmological distances inferred from the most recent observations of GRBs restrict the number of possibilities. At present, it appears that mergers of the components of binary systems containing pairs of neutron stars, or a neutron star–black hole pair, offer one of the few viable scenarios (e.g., Mészáros & Rees 1992).

While the recent results from *Beppo-SAX* are extremely exciting and encouraging, it is equally clear that further confirming measurements for a larger sample of burst counterparts are needed. For example, a small number of other GRBs (~ 4 – 6) have been detected with *Beppo-SAX*, for which *no* optical or radio counterparts have been discovered to date (e.g., Castro-Tirado et al. 1998). Paradoxically, some of these “noncounterpart” GRBs are much more intense gamma-ray events than either GRB 970228 and GRB 970508, for which counterparts were detected. It appears that each GRB still remains a unique event to a certain degree and caution must be exercised in deriving conclusions applicable to the phenomenon as a whole.

We now assess the implications of our present limits on the simultaneous microwave emission from GRBs and attempt to place them into context with the latest GRB counterpart results. Particularly popular classes of GRB models involve highly magnetized neutron stars or similar compact objects (e.g., Harding 1994). By analogy with pulsars and compact X-ray sources, both strong emitters in

the radio, a microwave counterpart to a GRB should not be excluded a priori. At the current level of understanding, an estimate of the microwave brightness of GRBs remains somewhat speculative. Particular attention is now being concentrated on variants of the relativistic fireball model (e.g., Paczyński & Rhoads 1993; Palmer 1993; Wijers et al. 1997). Palmer (1993), for example, estimates a GRB flux at radio wavelengths (< 10 GHz) of $\sim 10^8 \times (L_R/L_\gamma)$ Jy, with a range for the luminosity ratio L_R/L_γ from 10^{-2} to 10^{-7} , derived from pulsar X-ray emission. If the same scaling applies to microwaves, a positive detection of a GRB by the *COBE* DMR is more than a hypothetical possibility. At present, the detection by Frail et al. (1997) of millijansky-level emission at low radio frequencies from GRB 970508 provides the only firm counterpart data in this region of the spectrum. As pointed out by these same authors, the exact time of onset of radio emission from a GRB and its temporal behavior at the higher frequencies investigated here remain largely unconstrained, based on the single radio detection to date. While one may argue that the present limits on microwave emission do not themselves overly constrain the current GRB models, it is important to keep in mind that they do represent the first truly *simultaneous* counterpart measurement in this frequency regime and should be considered in future model predictions.

The upper limits of simultaneous microwave flux presented in this paper are comparable to or lower than the gamma-ray flux for many GRBs. A flux of 30 kJy over the frequency range from 30 to 90 GHz is equal to 1.8×10^{-8} ergs $\text{cm}^{-2} \text{s}^{-1}$. From plots in Meegan et al. (1996), we infer that about half of the GRBs have a peak flux of at least 3×10^{-7} ergs $\text{cm}^{-2} \text{s}^{-1}$ over a 1 s integration time. For 100 s time bins, our upper limits on mean microwave fluence are about 6.0×10^{-7} ergs $\text{cm}^{-2} \text{s}^{-1}$. In the 3B Catalog about 78% of the GRBs have a total fluence greater than this value, while about 50% have a total fluence of more than about 4 times this value.

While the cosmological interpretation of the origin of GRBs has gained strong support following the recent results from *Beppo-SAX*, it may yet be premature to completely abandon alternative scenarios proposed for the origin of GRBs. As reviewed by Lamb (1995), a sufficiently isotropic distribution of GRBs can also be expected if the gamma-ray emission arises from runaway neutron stars in an extended halo several hundred kiloparsecs in diameter surrounding our Galaxy. There are also a number of possible two-population distributions where the majority of the GRBs lie at cosmological distances or in an extended halo while a significant minority of sources come from an older disk population (see, for example, Hakkila et al. 1994 and references therein). If, as reported by some investigators (e.g., Efron & Petrosian 1995), some of the sources of GRBs give off repeated bursts, then the observed number of different sources may be considerably less than the number of individual GRBs and the limits on source location based on the observed GRB distribution will be weakened.

Allowing for these various alternative hypotheses, we note that the brightness temperature limit for incoherent nonthermal microwave emission from an expanding synchrotron source is about 10^{12} K. If the diameter of such a source is θ'' , a value of θ of order 0'.1 is necessary for detection with the DMR. The linear size of such a source would be about 10^8 AU at cosmological distances, 5×10^3 AU in an extended galactic halo, and about 5 AU for nearby stars

in the disk. By assuming an apparently superluminal expansion rate, we can anticipate that such an expanding source could be detectable with the DMR within 20 minutes after the GRB trigger time if the emission comes from nearby stars, but not in the other two cases.

If we consider coherent beamed emission as, for example, from a pulsar, then apparent brightness temperatures can reach up to 10^{23} K and source sizes can be almost 6 orders of magnitude smaller. Then, assuming that the microwave beaming is the same as the gamma-ray beaming, we could detect such sources with the DMR within 20 minutes if they lie in an extended galactic halo, or even if they were in distant (but not cosmologically distant) galaxies. Of course, one would need to devise a model whereby coherent microwave emission could occur over AU size volumes.

5. SUMMARY

Over the 8 month period 1991 April–December, the

COBE DMR instrument was pointing toward a number of GRBs at or within a few seconds of the BATSE trigger time. The upper limits of the simultaneous microwave flux, of order 7–42 kJy, imply that the energy emitted in microwaves is less than the energy emitted in gamma rays. This result seems more interesting physically for the case of GRB models in or near our Galaxy than for models where the GRBs originate at cosmological distances.

We wish to thank D. Leisawitz of the NSSDC and J. Newmark of the *COBE* guest investigator facility for providing the tapes of the DMR TOD. We also thank M. Briggs of the BATSE team for providing us with the burst location error models. We thank as well J. Mather, *COBE* Project Scientist, for early discussions regarding the feasibility of this project, and C. L. Bennett for helpful discussions. This work was supported in part by NASA grant NAG 5-2708 and by the Louisiana Board of Regents.

REFERENCES

- Ali, S., Schaefer, R. K., Limon, M., & Piccirillo, L. 1997, *ApJ*, 487, 114
 Bennett, C. L., et al. 1992, *ApJ*, 391, 466
 ———. 1994, *ApJ*, 436, 423
 ———. 1996, *ApJ*, 464, L1
 Bontekoe, Tj. R., Winkler, C., Stacy, J. G., & Jackson, P. D. 1995, *Ap&SS*, 231, 285
 Briggs, M., et al., 1998, in *AIP Conf. Proc. 428, Gamma-Ray Bursts: Fourth Huntsville Symposium*, ed. C. A. Meegan, R. D. Preece, & T. M. Koshut (New York: AIP), 104
 Castro-Tirado, A., et al., 1998, in *AIP Conf. Proc. 428, Gamma-Ray Bursts: Fourth Huntsville Symposium*, ed. C. A. Meegan, R. D. Preece, & T. M. Koshut (New York: AIP), 489
 Costa, E., et al. 1997, *Nature*, 387, 783
 Djorgovski, S. G., et al. 1997, *Nature*, 387, 876
 Efron, B., & Petrosian, V. 1995, *ApJ*, 449, 216
 Fishman, G. J. 1995, *PASP*, 107, 1145
 Fishman, G. J., et al. 1994, *ApJS*, 92, 229
 Frail, D. A., et al. 1997, *Nature*, 389, 261
 Greiner, J. 1995, *Ap&SS*, 231, 263
 Hakkila, J., et al. 1994, *ApJ*, 422, 659
 Hanlon, L. O., et al. 1994, *A&A*, 285, 161
 Harding, A. K. 1994, in *AIP Conf. Proc. 304, The Second Compton Symposium*, ed. C. E. Fichtel, N. Gehrels, & J. P. Norris (New York: AIP), 30
 Jackson, P. D., et al. 1992, in *Astronomical Data Analysis Software and Systems I*, ed. D. M. Worrall, C. Biemesderfer, & J. Barnes (San Francisco: ASP), 382
 Keegstra, P. B., et al. 1992, in *Astronomical Data Analysis Software and Systems I*, ed. D. M. Worrall, C. Biemesderfer, & J. Barnes (San Francisco: ASP), 530
 Kippen, R. M. 1995, Ph.D. thesis, Univ. New Hampshire
 Klebesadel, R., Strong, I., & Olsen, R. 1973, *ApJ*, 182, L85
 Lamb, D. Q. 1995, *PASP*, 107, 1152
 Meegan, C. A., et al. 1996, *ApJS*, 106, 65
 Mészáros, P., & Rees, M. J. 1992, *ApJ*, 397, 570
 Metzger, M. R., et al. 1997, *Nature*, 387, 878
 Norris, J. P., et al. 1995, *ApJ*, 439, 542
 Paczyński, B. 1995, *PASP*, 107, 1167
 Paczyński, B., & Rhoads, J. E. 1993, *ApJ*, 418, L5
 Palmer, D. M. 1993, *ApJ*, 418, L25
 Piro, L., Scarsi, L., & Butler, R. C., 1995, *Proc. SPIE*, 2517, 169
 Sahu, K. C., et al. 1997, *Nature*, 387, 476
 Schaefer, R. K., Ali, S., Limon, M., & Piccirillo, L. 1995, *Ap&SS*, 231, 331
 Smoot, G., et al. 1990, *ApJ*, 360, 685
 Stacy, J. G., Jackson, P. D., Bontekoe, R. Tj., & Winkler, C. 1996, in *AIP Conf. Proc. 384, Gamma-Ray Bursts: Third Huntsville Symposium*, ed. C. Kouveliotou, M. F. Briggs, & G. J. Fishman (New York: AIP), 702
 Taylor, G. B., et al. 1997, *Nature*, 389, 263
 van Paradijs, J., et al. 1997, *Nature*, 386, 686
 Vrba, F. J. 1996, in *AIP Conf. Proc. 384, Gamma-Ray Bursts: Third Huntsville Symposium*, ed. C. Kouveliotou, M. F. Briggs, & G. J. Fishman (New York: AIP), 565
 Waxman, E. 1997, *ApJ*, 485, L5
 Wijers, R. A. M. J., Rees, M. J., & Mészáros, P. 1997, *MNRAS*, 288, L51